J Vet Intern Med 2014;28:1280–1288

Effect of Dietary Nonstructural Carbohydrate Content on Activation of 5′-Adenosine Monophosphate-Activated Protein Kinase in Liver, Skeletal Muscle, and Digital Laminae of Lean and Obese Ponies

T.A. Burns, M.R. Watts, P.S. Weber, L.J. McCutcheon, R.J. Geor, and J.K. Belknap

Background: In EMS-associated laminitis, laminar failure may occur in response to energy failure related to insulin resistance (IR) or to the effect of hyperinsulinemia on laminar tissue. 5′-Adenosine-monophosphate-activated protein kinase (AMPK) is a marker of tissue energy deprivation, which may occur in IR.

Hypothesis/Objectives: To characterize tissue AMPK regulation in ponies subjected to a dietary carbohydrate (CHO) challenge.

Animals: Twenty-two mixed-breed ponies.

Methods: Immunohistochemistry and immunoblotting for total AMPK and phospho(P)-AMPK and RT-qPCR for AMPK-responsive genes were performed on laminar, liver, and skeletal muscle samples collected after a 7-day feeding protocol in which ponies stratified on body condition score (BCS; obese or lean) were fed either a low-CHO diet (ESC + starch, approximately 7% DM; n = 5 obese, 5 lean) or a high-CHO diet (ESC + starch, approximately 42% DM; n = 6 obese, 6 lean).

Results: 5′-Adenosine-monophosphate-activated protein kinase was immunolocalized to laminar keratinocytes, dermal constituents, and hepatocytes. A high-CHO diet resulted in significantly decreased laminar [P-AMPK] in lean ponies ($P = .03$), but no changes in skeletal muscle (lean, $P = .33$; obese, $P = .43$) or liver (lean, $P = .84$; obese, $P = .13$) [P-AMPK]. An inverse correlation existed between [blood glucose] and laminar [P-AMPK] in obese ponies on a high-CHO diet.

Conclusions and Clinical Importance: Laminar tissue exhibited a normal response to a high-CHO diet (decreased [P-AMPK]), whereas this response was not observed in liver and skeletal muscle in both lean (skeletal muscle, $P = .33$; liver, $P = .84$) and obese (skeletal muscle, $P = .43$; liver, $P = .13$) ponies.

Key words: Energy regulation; Equine metabolic syndrome; Insulin resistance; Laminitis.

Metabolic syndrome in humans is characterized by obesity-related systemic insulin resistance (IR). In systemic IR, tissues such as liver and skeletal muscle (which are the primary tissues mediating regulation of blood glucose concentration in response to insulin) do not regulate or respond normally to serum insulin or glucose concentrations, which can result in persistent hyperinsulinemia. Equine laminitis is associated with a diverse range of clinical diseases, from sepsis to endocrinopathies characterized by IR. Recent epidemiologic data suggest that laminitis associated with the equine metabolic syndrome (EMS; EMSAL) is now the most prevalent form of the disease.[1] Although IR and subsequent glucose deprivation have been suggested as potential mechanisms underlying laminar failure in EMSAL,[2] recent research suggests that glucose-related signaling in the laminar epithelium is not insulin-dependent.[3] Additionally, laminar basal epithelial cells (the cells that separate from their basement membrane during laminitis) do not appear to express the insulin receptor, suggesting that hyperinsulinemia may not directly affect these cells or may be activate alternate receptors (such as the insulin-like growth factor-1 receptor).[4] Although laminar energy dysregulation is thought to be involved in the pathophysiology of EMSAL,[2,5,6] the mechanism or mechanisms involved remain poorly characterized.

Abbreviations:

AMPK	5′-adenosine monophosphate-activated protein kinase
BCS	body condition score
CHO	carbohydrate
CON	control
DM	dry matter
EMSAL	equine metabolic syndrome–associated laminitis
EMS	equine metabolic syndrome
ESC	ethanol-soluble carbohydrate
FSIGTT	frequently sampled insulin-modified intravenous glucose tolerance test
HMS	human metabolic syndrome
IR	insulin resistant/insulin resistance
IS	insulin sensitivity/insulin sensitive
LBEC	laminar basal epithelial cell(s)
PEPCK	phosphoenolpyruvate carboxykinase
PGC-1α	peroxisome proliferator–activated receptor-γ coactivator 1-α
PPARγ	peroxisome proliferator-activated receptor-γ
RT-qPCR	real-time quantitative polymerase chain reaction

From The Ohio State University College of Veterinary Medicine, Columbus, OH (Burns, Watts, Belknap); and Michigan State University College of Veterinary Medicine, East Lansing, MI (Weber, McCutcheon, Geor).

Corresponding author: J.K. Belknap, DVM, PhD, DACVS, Department of Veterinary Clinical Sciences, College of Veterinary Medicine, The Ohio State University, 601 Vernon L. Tharp street, Columbus, OH 43210; e-mail: belknap.16@osu.edu.

Submitted August 15, 2013; Revised December 13, 2013; Accepted March 5, 2014.

DOI: 10.1111/jvim.12356

5′-Adenosine-monophosphate-activated protein kinase (AMPK) is a highly conserved enzymatic 'master regulator' of cellular energy status. AMPK activation is increased during cellular energy stress (increased AMP: ATP ratio), occurring primarily by phosphorylation of a highly conserved threonine residue on the α-subunit (Thr172). This phosphorylation event results in downstream effects on intermediary metabolism that favor ATP production and limit ATP consumption.[7] AMPK activation improves systemic insulin sensitivity by increasing lipid oxidation, mitochondrial biogenesis, glucose uptake, and other mechanisms. Consequently, AMPK has emerged as an attractive therapeutic target for the treatment of metabolic syndrome in humans (HMS).[8] Metformin, a functional AMPK agonist, is an orally bioavailable biguanide that has been used as an antihyperglycemic and insulin-sensitizing medication in the treatment of HMS and Type II diabetes mellitus.[9] In IR humans, metformin treatment (AMPK agonism) results in enhanced tissue glucose uptake, decreased glycogen synthesis and lipogenesis, increased β-oxidation, and improved systemic insulin sensitivity.[10] These changes are associated with altered expression of several genes with roles in carbohydrate and lipid metabolism and mitochondrial biogenesis (including PEPCK, PGC-1α, AMPKα, and PPARγ).[11,12]

Although metformin has been used empirically to treat EMS patients,[13] little is known about the biologic behavior of the drug or, more importantly, its target (AMPK) in equids. Most published studies of metformin in equine systems describe its pharmacokinetics in various populations, in which its oral bioavailability is reportedly low (4–7%).[14–17] Although initial pharmacodynamic information has been reported regarding metformin's activity in equine systems,[15,17] information regarding AMPK and its activation and inhibition in tissues of interest in EMS and EMSAL (eg, digital laminae, skeletal muscle, liver) has not been reported to date. Thus, it is critical to evaluate AMPK signaling in a model of EMSAL to determine whether or not AMPK agonism represents a sound therapeutic target for improving systemic insulin sensitivity and treating or preventing EMSAL in horses and ponies. Therefore, we determined the activation state of AMPK and the regulation of AMPK-associated genes in 2 primary insulin-responsive tissues (liver and skeletal muscle) and in the digital laminae of ponies subjected to a dietary carbohydrate (ethanol-soluble carbohydrate [ESC] + starch) challenge meant to mimic acute pasture exposure.

Materials and Methods

Experimental Animals

Archived samples from 22 mixed-breed ponies (body weight, 270.9 ± 74.4 kg; age [lean], 9.2 ± 3.5 years; age [obese], 11 ± 3.8 years) were used for this study. All animals received humane treatment in accordance with an animal care and use protocol approved by the MSU Institutional Animal Care and Use Committee. Feedstuffs used in the protocol were analyzed for ESC + starch content by a commercial laboratory.[a] All ponies obtained for the study were examined by a licensed veterinarian and deemed healthy based on the results of physical examination, complete blood count, and serum biochemistry. Ponies were divided into 4 groups based on BCS: lean, low-CHO (n = 5); obese, low CHO (n = 5); lean, high-CHO (n = 6); and obese, high-CHO (n = 6). All BCS scoring was performed independently by 2 individuals; lean animals were those assigned a BCS of ≤4/9, and obese animals were those assigned a BCS of ≥7/9.[18]

Ponies were housed in dirt lots and conditioned to a diet of hay chop (7% starch and ethanol-soluble carbohydrate on a dry matter [DM] basis) for 4 weeks before the experimental feeding protocol. Ponies were fed 2.5% of their body weight in hay chop per day, divided into 2 feedings (7 AM and 6 PM EST). After conditioning, all ponies continued to receive hay chop at the previously fed rate; this was the only feedstuff fed to ponies in the low-CHO groups. Ponies on the high-CHO diet received supplemental sweet feed (1.5% body weight per day, divided into 3 daily feedings at 7 AM, 12 PM, and 6 PM EST) and oligofructose[b] (2 g/kg added to hay chop [fed at 2.5% BW]) for a period of 7 days. The mean ESC + starch consumption of ponies in the low-CHO groups was approximately 1.8 g/kg/d, whereas that of ponies in the high-CHO groups was approximately 8 g/kg/d. Serum insulin and glucose measurements were performed as previously reported.[4] All ponies were fed low-CHO hay chop overnight before blood collection, with complete withdrawal of all feed for 2 hours immediately before sampling.

After the 7-day experimental period, ponies were euthanized by IV overdose of pentobarbital sodium and phenytoin sodium[c] (20 mg/kg IV). The right front foot of each animal was removed by disarticulation of the metacarpophalangeal joint immediately after euthanasia, and 1.5-cm sagittal sections of the dorsal digit were cut with a band saw. After dissection of the digital laminae from the hoof wall and third phalanx, sections of laminae were snap-frozen in liquid nitrogen or fixed in 10% neutral buffered formalin; all laminar samples were processed within 15 minutes of euthanasia. Samples of skeletal muscle (middle gluteal muscle) and liver were similarly collected and processed. All formalin-fixed samples were transferred to 70% ethanol after 48 hours, where they were stored until paraffin embedding. Frozen samples were stored at −80°C until analysis (approximately 4 months after sample collection).

Immunohistochemistry

Formalin-fixed laminar and liver tissue samples were embedded in paraffin and sectioned at 5 μm for immunohistochemistry. Primary antibodies evaluated for immunohistochemical detection of P-AMPK performed poorly in equine tissue; therefore, the immunohistochemistry described here represents tissue localization of total AMPK. Staining of tissue samples was performed as previously reported.[19] Briefly, sections were deparaffinized and incubated in a rabbit monoclonal antihuman AMPK-β1/2 primary antibody[d] (1 : 100, incubated overnight at 4°C). Detection of immunoreactivity was performed using a goat/antirabbit IgG-HRP secondary antibody,[e] an immunoperoxidase system,[f] and 3,3′-diaminobenzidine (DAB) substrate.[g] The distribution of total-AMPK (+) cells in all liver and digital laminar sections was evaluated by light microscopy by a single blinded observer (TAB), and the results were qualitatively described.

Western Immunoblotting

The concentration of phosphorylated and total AMPK in liver, skeletal muscle, and laminar tissue homogenates was assessed by Western immunoblotting performed as described previously.[20] Briefly, protein samples (approximately 300 mg tissue per sample) were prepared in 5 mL of lysis buffer[h] with

added protease and phosphatase inhibitors and quantitated using the Bradford method. Protein samples (20 μg/sample) were denatured by boiling for 5 minutes in β-mercaptoethanol and sodium dodecyl sulfate (β-ME/SDS) buffer, separated on an 8% polyacrylamide gel, and transferred to a polyvinylidene difluoride (PVDF) membrane. The membrane was blocked for 1 hour with 5% nonfat dry milk in Tris-buffered saline (TBS) with Tween-20 (0.1% v/v Tween-20 in TBS; TBST) at room temperature with rocking. The membrane then was incubated with primary antibody[i,j] (1 : 1000 in blocking buffer [5% nonfat milk in TBST]) overnight at 4°C. The membrane was washed 5 times with 0.1% TBST as before. Goat/antirabbit IgG-HRP secondary antibody[g] was diluted 1 : 5000 in 5% nonfat milk and incubated with the membrane for 1 hour at room temperature with rocking. The membrane was washed 5 times with 0.1% TBST and developed for 5 minutes using a chemiluminescent substrate.[k] The membrane first was probed for P-AMPK,[k] then stripped and reprobed sequentially for total AMPK[l] and β-actin.[l] Luminescence was measured using a computer software program,[m] and signal strength was determined using net phospho-AMPK band intensity divided by the total AMPK and β-actin band intensities.

RNA Isolation, cDNA Synthesis, and Real-Time Quantitative Polymerase Chain Reaction (RT-qPCR)

Homogenates were made from each tissue sample (approximately 100 mg) with a tissue disruptor,[n] and total RNA was extracted using a commercially available kit.[o] Messenger RNA (mRNA) then was isolated from total RNA utilizing poly-A tail hybridization[p] and quantified.[q] Complementary DNA (cDNA) was synthesized from mRNA isolated from each sample using reverse transcription[r] and stored at −20°C until used for real-time quantitative polymerase chain reaction (RT-qPCR) analysis.

A thermocycler[s] was used to perform RT-qPCR. Amplification was quantified against external standards using fluorescent format for SYBR Green I as previously described.[21,22] Primers for peroxisome proliferator-activated receptor-γ (PPARγ), peroxisome proliferator-activated receptor-γ coactivator 1-α (PGC1α), AMPKα, phosphoenolpyruvate carboxykinase (PEPCK), and the housekeeping genes β-actin and β_2-microglobulin were designed against equine-specific gene sequences (using exon sequence spanning an intron) using computer programs as previously described[21,23,24]; these primers subsequently were used for amplification of the respective genes of interest. Standard curves for quantification of mRNA concentration in laminar tissue samples were generated using serial dilutions of a linearized vector[t] containing an insert of each amplified cDNA fragment (identity confirmed by nucleic acid sequencing). All PCR assays were run in duplicate, including liver, laminar, and skeletal muscle samples; standards of known concentration; and, negative control samples.

RT-qPCR data from 2 housekeeping genes (β-actin and β_2-microglobulin) were entered into a commercially available computer program[u] to test each gene's suitability as a housekeeping gene for the equine laminar tissue samples. Because both genes were determined to be satisfactory by the program, a geometric mean was obtained from the 2 genes' data to generate a normalization factor for gene expression from each separate tissue sample (liver, skeletal muscle, and digital laminae from each individual pony). Gene expression data from the genes of interest then were normalized using this factor for each sample.

Data Analysis

Data analysis was performed using a statistical software program.[v] All data were assessed for normality by the Shapiro-Wilk and D'Agostino and Pearson omnibus normality tests. mRNA concentration data were analyzed with a 2-way analysis of variance followed by a Bonferroni posttest, as appropriate. Protein concentration data were analyzed with a Student's *t*-test or nonparametric equivalent. Because of the limited number of samples that could be loaded on a single electrophoretic gel, protein results from lean and obese ponies were not compared with each other; only the effect of diet was evaluated. Correlations among normally distributed data sets were evaluated by calculation of Pearson's *r*. Statistical significance was accepted at $P < .05$. Data are expressed as mean ± standard deviation unless otherwise indicated.

Results

Serum Insulin and Glucose Concentrations

Basal serum insulin and glucose concentrations on day 7 of the experimental protocol were increased in response to high-CHO feeding in the obese ponies (Table 1). A significant inverse correlation between day 7 blood glucose concentration and digital laminar phospho-(Thr172) AMPKα concentration was observed in obese ponies ($r = -0.64$; $P = .05$), a finding that was not observed in lean ponies ($P = .47$).

Immunohistochemistry

The cellular and subcellular immunolocalization of the β-subunit of the AMPK enzymatic complex was evaluated qualitatively by histochemical staining of liver and digital laminar tissue. No effect of diet or BCS on the quantity or distribution of AMPK was readily apparent in either tissue, but this was a subjective assessment and would be considered poorly sensitive for detection of subtle effects. Within the digital laminae, most cell types expressed AMPK, including laminar keratinocytes (including laminar basal epithelial cells; LBEC), vascular endothelial and smooth muscle cells, and dermal mesenchymal cells (presumed to be fibroblasts and possibly tissue macrophages). Within the liver, most AMPK(+) cells were hepatic

Table 1. Serum insulin and glucose concentration data from Day 7 of experimental protocol.

	LEAN CON	LEANCHO	OB CON	OBCHO
Serum [insulin] (mIU/L)*	6.6^{a} (2.63–11.23)	124.4^{a} (45.1–653.8)	27.2^{a} (12.2–29.1)	641.0^{b} (226.0–811.0)
Blood [glucose] (mg/dL)†	78.4^{c} (61.2–98.4)	82.9^{c} (74.6–80.4)	66.9^{c} (48.8–80.4)	113.7^{d} (103.3–161.6)

Across each row, columns bearing different superscripts are statistically different. Data presented as median (interquartile range).
*$P = .022$.
†$P = .002$.

sinusoidal epithelial cells, with little staining of endothelial cells or leukocytes. In digital laminae, a rim of perinuclear stain uptake was noted in many laminar keratinocytes; and, in the liver, a granular appearance to hepatocyte cytoplasmic staining was observed (consistent with AMPK's reported association with glycogen[25]; see Fig 1). Although the intensity or localization of hepatic AMPK immunohistochemical staining was not observed to change with relatively high-CHO feeding, animals fed this diet appeared to have increased cytoplasmic clearing visible within hepatocytes (a finding consistent with, but not diagnostic of, lipid accumulation; Fig 1).

Western Immunoblotting

Phospho-(Thr 172) AMPKα concentrations in digital laminar tissue were significantly decreased in lean ponies fed the high-CHO diet ($P = .03$). In contrast, phospho-(Thr 172) AMPKα concentrations did not change in liver and skeletal muscle in response to the high-CHO diet in both lean (skeletal muscle, $P = .33$; liver, $P = .84$) and obese ponies (skeletal muscle, $P = .43$; liver, $P = .13$; see Fig 2).

RT-qPCR

The mRNA concentration of PEPCK was significantly increased in skeletal muscle in response to high-CHO feeding in both lean and obese ponies ($P = .02$); no effect was observed in digital laminae ($P = .37$) or liver ($P = .58$). No effect of diet or body condition on the gene expression of PPARγ, PGC1α, or AMPKα was observed in liver, skeletal muscle, or digital laminar tissue ($P > .05$, all analytes; Fig 3).

Discussion

Since the first reports of experimental laminitis induction by prolonged systemic insulin and glucose infusion were published,[5,6] much speculation has occurred regarding the most important and relevant pathophysiologic mechanisms by which laminitis develops in this setting. Initial reports suggested that laminar IR may exist, resulting in chronic glucose (carbon substrate) deprivation at the cellular level, energy failure, and dermoepidermal separation (based on in vitro experiments using laminar explants incubated in glucose-free media for prolonged periods and subjected to mechanical distraction).[2] However, more recent publications have suggested that the digital laminar tissue is relatively insulin-insensitive or insulin-independent. Asplin et al. reported little increase in glucose uptake by laminar tissue explants from normal horses in response to incubation with insulin, as well as providing evidence that GLUT1 (instead of the insulin-responsive GLUT4) may be the predominant glucose transporter present in laminar tissue homogenates in both normal and chronically laminitic horses.[3] Furthermore, recent work has documented little evidence of insulin receptor expression on laminar keratinocytes of lean and obese ponies, a finding that does not appear to be affected significantly by high-CHO feeding.[4] Finally, results of the current study, establishing

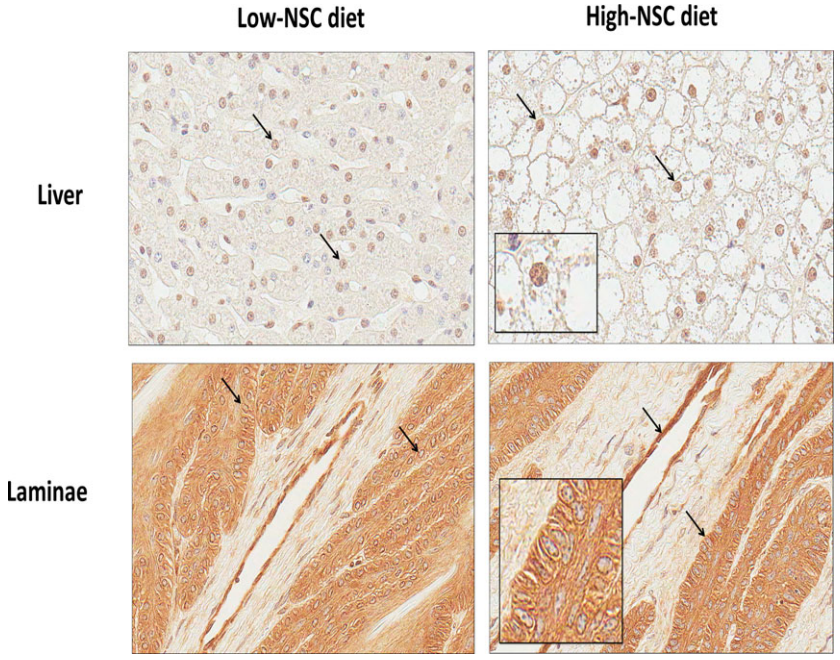

Fig 1. Immunohistochemical staining of liver and digital laminae against the β-subunit of 5′-adenosine-monophosphate-activated protein kinase (AMPK) (total AMPK). Note the distinct perinuclear staining (arrows; insets) in both liver and laminae, and the granular cytoplasmic staining in liver (consistent with reported association of the complex with glycogen). All images are at 40× magnification; images on the left are from animals fed a low-CHO diet, and those on the right are from animals fed a high-CHO diet.

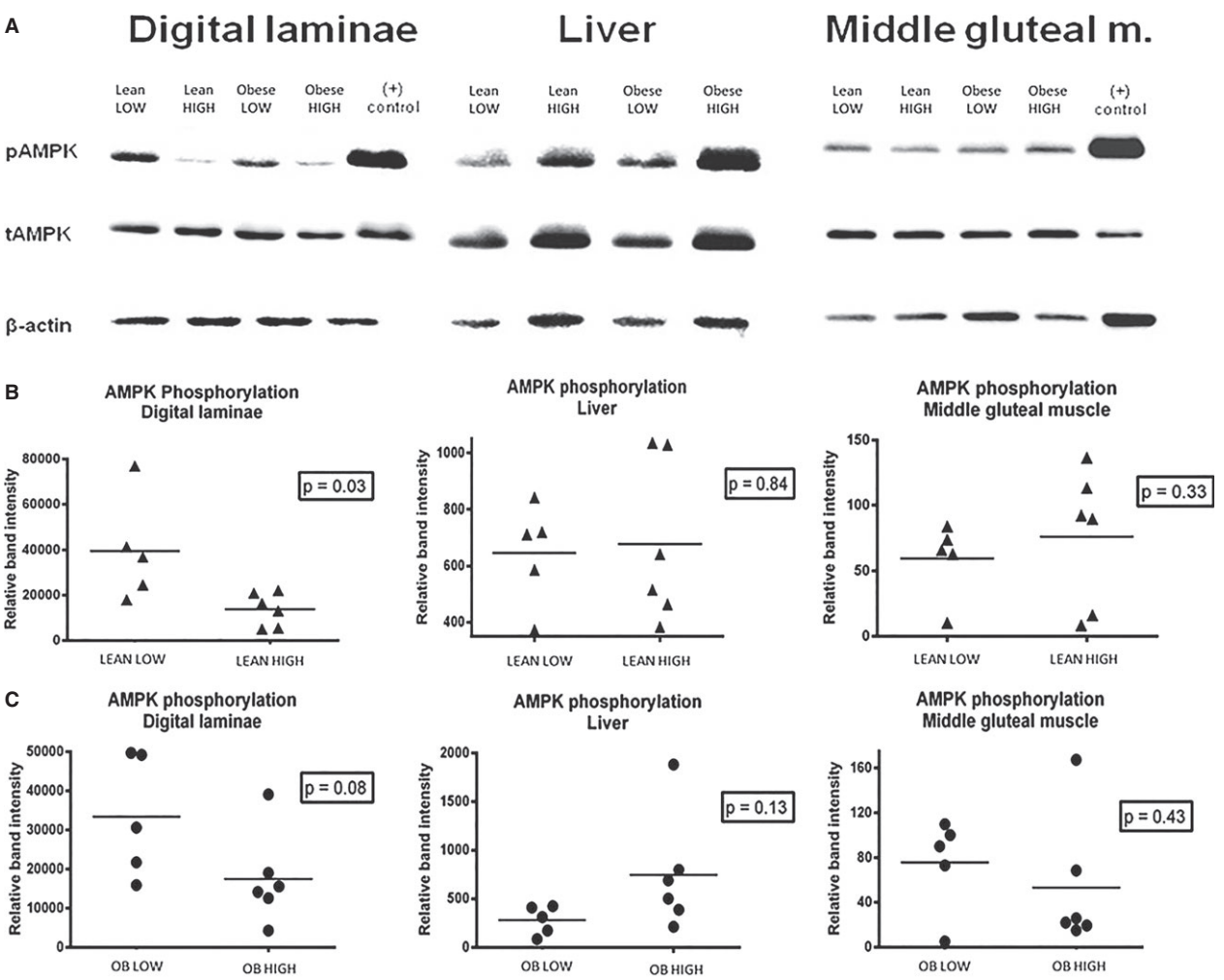

Fig 2. 5′-Adenosine-monophosphate-activated protein kinase (AMPK) activating phosphorylation in response to high-CHO feeding in digital laminae, liver, and skeletal muscle of obese and lean ponies. Representative Western blot images from pooled protein samples are shown in panel **(A)**; panels **(B)** and **(C)** display densitometry data from Western blots of individual animal samples assessing AMPK phosphorylation in laminae, liver, and skeletal muscle of lean (B, triangles) and obese ponies (C, circles). While P-AMPK decreases in laminar tissue in response to high-CHO feeding (suggesting insulin sensitivity, or insulin independence of this tissue), this pattern is not observed in liver or skeletal muscle. Data are derived from the following ratio of immunoblot band densities: P-AMPK/tAMPK/β-actin. P-AMPK, phosphorylated AMPK; tAMPK, total AMPK; CON, control diet; CHO, carbohydrate challenge diet; OB, obese.

decreased laminar P-AMPK concentrations in obese and lean ponies consuming a high-CHO diet, are not consistent with digital laminar tissue IR, nor are they consistent with laminar energy deprivation or stress, where a robust increase in P-AMPK concentrations induced by an increasing AMP:ATP ratio would be expected as cellular energy stores are depleted.[26] Laminar AMPK phosphorylation also was noted to be inversely correlated with blood glucose concentrations (but not with insulin concentrations) in obese ponies. This finding provides additional support for the concept that transcellular glucose flux may be more important in the pathophysiology of EMSAL than insulin signaling.

Vascular events also have been suggested to be involved in the pathogenesis of laminitis,[27] with hypoperfusion and subsequent energy deprivation and hypoxia proposed as important contributors to dermo-epidermal separation.[28,29] Although systemic hypertension has been reported in IR ponies at risk for pasture-associated laminitis,[30] the role that insulin and IR play in the vasculature of the equine digit and laminar perfusion is poorly described. The ponies of the study reported here became hyperinsulinemic in response to high-CHO feeding (and many were systemically IR [4]), but evidence of hypoxia and energy stress was not detected in their digital laminae. Hypoxia is reported to result in potent AMPK activation in several species.[31–34] As mentioned above, one would expect to observe increased digital laminar concentrations of P-AMPK in response to energy deprivation if hypoperfusion and hypoxia were present, an effect that was not observed in this study. If anything, the results of this study support digital vasodilatation, with enhanced glucose delivery to the laminae. These findings, along with the findings of previous investigations, suggest that although increased

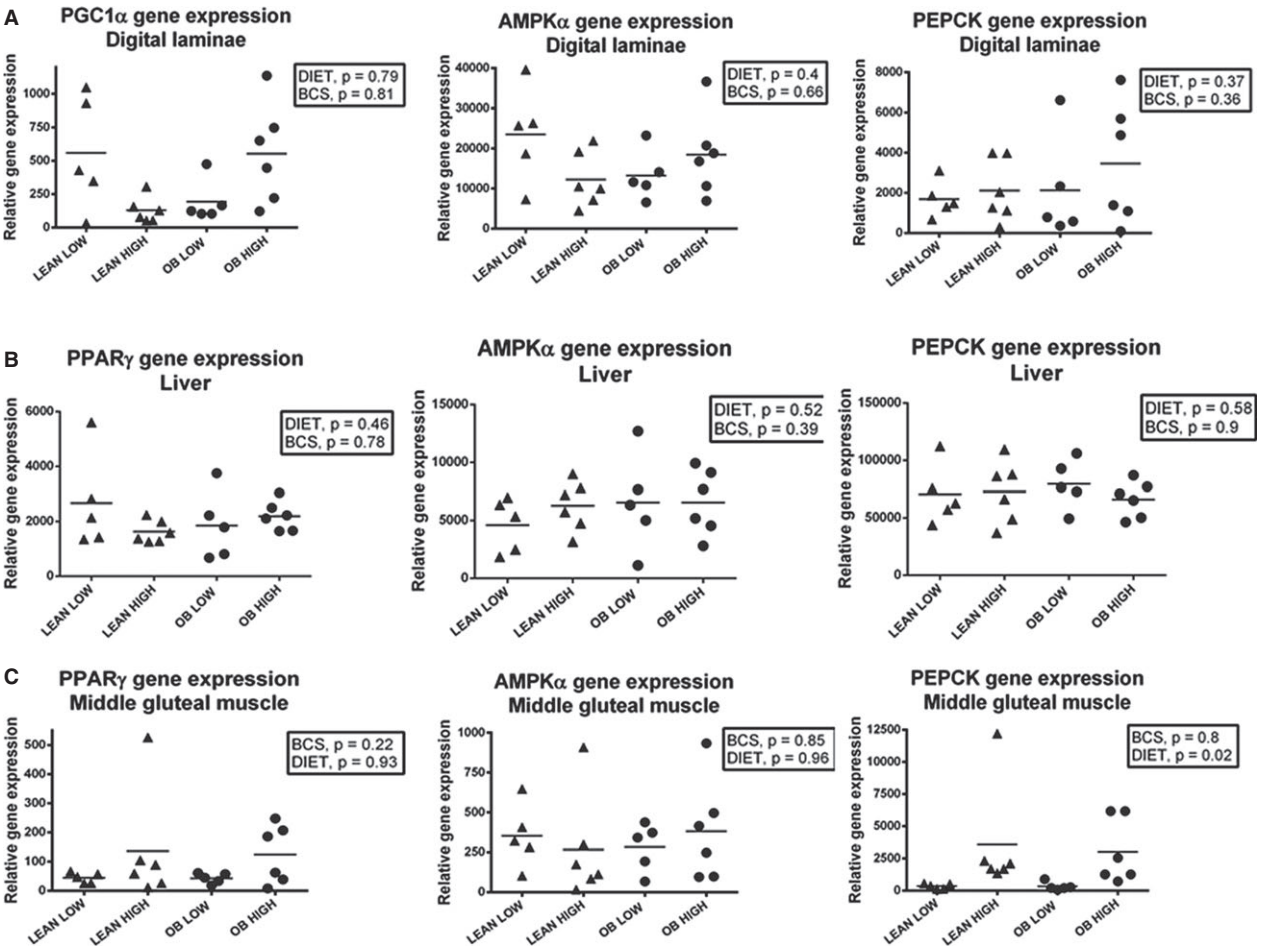

Fig 3. RT-qPCR data from digital laminae (row **A**), liver (row **B**), and skeletal muscle (row **C**) for genes regulated downstream of 5′-adenosine-monophosphate-activated protein kinase (AMPK) activation in lean (triangles) and obese (circles) ponies fed low- or high-CHO diets. The mRNA concentration of PEPCK was significantly increased in skeletal muscle in response to high-carbohydrate feeding in both lean and obese ponies; no effect was observed in digital laminae or liver. No effect of diet or body condition on the gene expression of PPARγ, PGC1α, or AMPKα was observed in liver, skeletal muscle, or digital laminar tissue. PPARγ, peroxisome proliferator-activated receptor-γ; PGC1α, peroxisome proliferator-activated receptor-γ coactivator 1-α; AMPKα, adenosine monophosphate-activated protein kinase α-subunit; PEPCK, phosphoenolpyruvate carboxykinase; OB, obese; LOW, low-CHO diet; HIGH, high-CHO diet.

vasomotor tone may be present in equids with EMS, it is unlikely to play a primary role in the pathogenesis of EMSAL.

In addition to its well-characterized roles in energy regulation, AMPK more recently has been shown to be important in the maintenance and dynamic repair of intercellular tight junctions,[35,36] enhancement of cell-cell contacts,[37] induction of phenotypic differentiation, and determination of cell polarity.[38–40] Although the net effects of AMPK activation or inhibition on the function of the equine LBEC are unknown, it may play a role in this highly polarized, structurally critical cell type. The cytoskeletal interactions of LBEC are crucial for regulation and integrity of adhesion complexes such as hemidesmosomes (HD), which attach to the underlying dermis (associated with the distal phalanx) on the basal side of the cell allowing suspension of the distal phalanx by the hoof capsule.[41,42] AMPK thus may provide an attractive link among dietary CHO content, insulin sensitivity (effects on blood insulin and glucose concentrations), and laminar epithelial dysfunction leading to LBEC dysadhesion.

The pattern of AMPK activation noted in liver and skeletal muscle is supportive of an unchanged AMP/ATP ratio in these tissues, which would not be expected in the face of increased dietary CHO intake if tissue glucose uptake paralleled dietary intake.[43,44] IR at the tissue level may result in poor correlation between postprandial glycemia and intracellular translocation of glucose. Alternatively or additionally, ectopic lipid deposition and resultant mitochondrial dysfunction may be associated with decreased ATP production.[45–48] As systemic IR develops in the obese equid (with primary contributions from liver and skeletal muscle IR), ingestion of a high-CHO diet may result in persistent postprandial hyperglycemia and subsequent increased transcellular glucose flux in the digital laminae and other noninsulin-dependent tissues, such

as CNS and kidney. Decreased AMPK activation in the laminae then may mediate downstream effects on cell polarity and cytoskeletal organization that contribute to EMSAL.

Inhibition of laminar AMPK activation (such as seen here in response to high-CHO feeding) also may alter the differentiation phenotype and adherence of LBEC, as has been shown in other systems.[35,36,39] Decreased AMPK activation has been reported to result in activation of mTORC1/p70S6K/RPS6 signaling (known to be important in the poorly differentiated, less adhesive phenotype of tumor cells).[49,50] We recently have found evidence of laminar RPS6 activation in this same model (Belknap et al, unpublished data), and it is possible that AMPK may work through this mechanism to result in a less adhesive LBEC and ultimately result in structural failure of the laminae.

AMPK is known to phosphorylate and alter the activity of transcription factors controlling the expression of several target genes involved in carbohydrate and lipid metabolism and mitochondrial biogenesis.[11] However, little evidence of upregulation of AMPK target genes was detected in this study, inasmuch as no changes in mRNA concentrations of PPARγ, PGC-1α, or AMPKα were observed in any tissue examined in response to high-CHO feeding. PEPCK expression was unchanged in liver and digital laminae in response to dietary CHO, but a significant increase in skeletal muscle PEPCK mRNA concentration was observed in response to high-CHO feeding. PEPCK catalyzes the first committed step in gluconeogenesis, and its gene expression is reportedly repressed by actions of insulin[51] and AMPK (repression by insulin is reportedly dominant).[52] The observed upregulation of PEPCK gene expression in skeletal muscle in this study may be a consequence of IR in this tissue.

The results of this study do not support energy deprivation secondary to laminar IR as a central mechanism in EMSAL. In fact, decreased AMPK activation in the laminae associated with high-CHO feeding suggests tissue insulin sensitivity, insulin independence or both with respect to laminar glucose uptake. Furthermore, the presence of decreased laminar P-AMPK argues against substantial tissue ischemia in this setting, because AMPK activation would be expected in a tissue deprived of nutrients in this manner. Thus, whereas skeletal muscle and liver probably contribute to systemic IR and hyperinsulinemia in EMS, laminar dysfunction and injury in EMS are more likely because of the local effects of hyperinsulinemia or cellular glucose flux, and not local IR or energy failure.

Footnotes

[a] Equi-Analytical Laboratories, Ithaca, NY
[b] BENEO-Orafti, Tienen, Belgium
[c] Fatal Plus; Vortech Pharmaceuticals Ltd, Dearborn, MI
[d] cs4150; Cell Signaling Technology Inc, Danvers, MA
[e] cs7074; Cell Signaling Technology Inc
[f] Vectastain ABC system; Vector Laboratories, Burlingame, CA
[g] DAB peroxidase substrate kit; Vector Laboratories
[h] M-PER; Thermo Fisher Scientific, Inc, Rockford, IL
[i] cs2535 (phospho-Thr172 AMPK); Cell Signaling Technology Inc
[j] cs5831 (β1/2 AMPK subunit); Cell Signaling Technology Inc
[k] SuperSignal West Femto, Thermo Fisher Scientific, Inc
[l] sc1616; Santa Cruz Biotechnology, Inc, Dallas, TX
[m] Carestream Health, Inc, Rochester, NY
[n] Tissue-Ruptor; QIAGEN, Valencia, CA
[o] Absolutely RNA Miniprep kit; Agilent Technologies, Stratagene Products Division, La Jolla, CA
[p] mRNA extraction kit; Roche Applied Science, Indianapolis, IN
[q] NanoDrop Spectrophotometer; Thermo Scientific, Wilmington, DE
[r] Retroscript; Ambion, Inc, Austin, TX
[s] Roche 480; Roche Applied Science, Indianapolis, IN
[t] TOPO TA Cloning Kit; Invitrogen, Carlsbad, CA
[u] geNorm; Ghent University, Ghent, Belgium
[v] GraphPad Prism 5; GraphPad Software, La Jolla, CA

Acknowledgments

The authors gratefully acknowledge the staff members of the Diagnostic Center for Population and Animal Health of the Michigan State University College of Veterinary Medicine for their assistance with sample collection for this project.

Portions of this study were presented in abstract form at the Havemeyer Equine Laminitis Workshop II (April 2012), the Forum of the American College of Veterinary Internal Medicine (June 2012), and the 2nd Annual Equine Endocrinology Summit (October 2012). This work was supported by grants from the Michigan State University College of Veterinary Medicine and the Morris Animal Foundation.

Conflict of Interest Declaration: Authors disclose no conflict of interest.

References

1. USDA-NAHMS. Lameness and laminitis in US horses. United States Department of Agriculture National Animal Health Monitoring System. 2000; April(#N318.0400).

2. French KR, Pollitt CC. Equine laminitis: Glucose deprivation and MMP activation induce dermo-epidermal separation in vitro. Equine Vet J 2004;36:261–266.

3. Asplin KE, Curlewis JD, McGowan CM, et al. Glucose transport in the equine hoof. Equine Vet J 2011;43:196–201.

4. Burns TA, Watts MR, Weber PS, et al. Distribution of insulin receptor and insulin-like growth factor-1 receptor in the digital laminae of mixed-breed ponies: An immunohistochemical study. Equine Vet J 2013;45(3):326–332.

5. de Laat MA, McGowan CM, Sillence MN, Pollitt CC. Equine laminitis: Induced by 48 h hyperinsulinaemia in standardbred horses. Equine Vet J 2010;42:129–135.

6. Asplin KE, Sillence MN, Pollitt CC, McGowan CM. Induction of laminitis by prolonged hyperinsulinaemia in clinically normal ponies. Vet J 2007;174:530–535.

7. Shirwany NA, Zou MH. AMPK in cardiovascular health and disease. Acta Pharmacol Sin 2010;31:1075–1084.

8. Yang YM, Han CY, Kim YJ, Kim SG. AMPK-associated signaling to bridge the gap between fuel metabolism and hepatocyte viability. World J Gastroenterol 2010;16:3731–3742.

9. Mehnert H. Metformin, the rebirth of a biguanide: Mechanism of action and place in the prevention and treatment of insulin resistance. Exp Clin Endocrinol Diabetes 2001;109(Suppl 2): S259–S264.

10. Schultze SM, Hemmings BA, Niessen M, Tschopp O. PI3K/AKT, MAPK and AMPK signalling: Protein kinases in glucose homeostasis. Expert Rev Mol Med 2012;11:e1. doi:10.1017/S1462399411002109.

11. McGee SL, Hargreaves M. AMPK-mediated regulation of transcription in skeletal muscle. Clin Sci (Lond) 2010;118:507–518.

12. Leff T. AMP-activated protein kinase regulates gene expression by direct phosphorylation of nuclear proteins. Biochem Soc Trans 2003;31:224–227.

13. Durham AE, Rendle DI, Newton JE. The effect of metformin on measurements of insulin sensitivity and beta cell response in 18 horses and ponies with insulin resistance. Equine Vet J 2008;40:493–500.

14. Hustace JL, Firshman AM, Mata JE. Pharmacokinetics and bioavailability of metformin in horses. Am J Vet Res 2009;70:665–668.

15. Rendle DI, Rutledge F, Hughes KJ, et al. Effects of metformin hydrochloride on blood glucose and insulin responses to oral dextrose in horses. Equine Vet J 2013;45(6):751–754; doi:10.1111/evj.12068.

16. Tinworth KD, Edwards S, Noble GK, et al. Pharmacokinetics of metformin after enteral administration in insulin-resistant ponies. Am J Vet Res 2010;71:1201–1206.

17. Tinworth KD, Boston RC, Harris PA, et al. The effect of oral metformin on insulin sensitivity in insulin-resistant ponies. Vet J 2012;191:79–84.

18. Henneke DR, Potter GD, Kreider JL, Yeates BF. Relationship between condition score, physical measurements and body fat percentage in mares. Equine Vet J 1983;15:371–372.

19. Burns TA, Westerman T, Nuovo GJ, et al. Role of oxidative tissue injury in the pathophysiology of experimentally induced equine laminitis: A comparison of 2 models. J Vet Intern Med 2011;25:540–548.

20. Blikslager AT, Yin C, Cochran AM, et al. Cyclooxygenase expression in the early stages of equine laminitis: A cytologic study. J Vet Intern Med 2006;20:1191–1196.

21. Waguespack RW, Cochran A, Belknap JK. Expression of the cyclooxygenase isoforms in the prodromal stage of black walnut-induced laminitis in horses. Am J Vet Res 2004;65:1724–1729.

22. Waguespack RW, Kemppainen RJ, Cochran A, et al. Increased expression of MAIL, a cytokine-associated nuclear protein, in the prodromal stage of black walnut-induced laminitis. Equine Vet J 2004;36:285–291.

23. Leise BS, Faleiros RR, Watts M, et al. Laminar inflammatory gene expression in the carbohydrate overload model of equine laminitis. Equine Vet J 2011;43:54–61.

24. Burns TA, Geor RJ, Mudge MC, et al. Proinflammatory cytokine and chemokine gene expression profiles in subcutaneous and visceral adipose tissue depots of insulin-resistant and insulin-sensitive light breed horses. J Vet Intern Med 2010;24:932–939.

25. McBride A, Hardie DG. AMP-activated protein kinase–a sensor of glycogen as well as AMP and ATP? Acta Physiol (Oxf) 2009;196:99–113.

26. Towler MC, Hardie DG. AMP-activated protein kinase in metabolic control and insulin signaling. Circ Res 2009;100:328–341.

27. Hood DM, Grosenbaugh DA, Mostafa MB, et al. The role of vascular mechanisms in the development of acute equine laminitis. J Vet Intern Med 1993;7:228–234.

28. Venugopal CS, Eades S, Holmes EP, Beadle RE. Insulin resistance in equine digital vessel rings: An in vitro model to study vascular dysfunction in equine laminitis. Equine Vet J 2011;43:744–749.

29. Robertson TP, Bailey SR, Peroni JF. Equine laminitis: A journey to the dark side of venous. Vet Immunol Immunopathol 2009;129:164–166.

30. Bailey SR, Habershon-Butcher JL, Ransom KJ, et al. Hypertension and insulin resistance in a mixed-breed population of ponies predisposed to laminitis. Am J Vet Res 2008;69:122–129.

31. Gusarova GA, Trejo HE, Dada LA, et al. Hypoxia leads to Na, K-ATPase downregulation via Ca(2+) release-activated Ca(2+) channels and AMPK activation. Mol Cell Biol 2011;31:3546–3556.

32. Mungai PT, Waypa GB, Jairaman A, et al. Hypoxia triggers AMPK activation through reactive oxygen species-mediated activation of calcium release-activated calcium channels. Mol Cell Biol 2011;31:3531–3545.

33. LaRue BL, Padilla PA. Environmental and genetic preconditioning for long-term anoxia responses requires AMPK in *Caenorhabditis elegans*. PLoS ONE 2011;6:e16790.

34. Yan H, Zhang DX, Shi X, et al. Activation of the prolyl-hydroxylase oxygen-sensing signal cascade leads to AMPK activation in cardiomyocytes. J Cell Mol Med 2012;16:2049–2059.

35. Miranda L, Carpentier S, Platek A, et al. AMP-activated protein kinase induces actin cytoskeleton reorganization in epithelial cells. Biochem Biophys Res Commun 2010;396:656–661.

36. Zhang L, Li J, Young LH, Caplan MJ. AMP-activated protein kinase regulates the assembly of epithelial tight junctions. Proc Natl Acad Sci USA 2006;103:17272–17277.

37. Kim HS, Kim MJ, Kim EJ, et al. Berberine-induced AMPK activation inhibits the metastatic potential of melanoma cells via reduction of ERK activity and COX-2 protein expression. Biochem Pharmacol 2012;83:385–394.

38. Lo B, Strasser G, Sagolla M, et al. Lkb1 regulates organogenesis and early oncogenesis along AMPK-dependent and -independent pathways. J Cell Biol 2012;199:1117–1130.

39. Jansen M, Ten Klooster JP, Offerhaus GJ, Clevers H. LKB1 and AMPK family signaling: The intimate link between cell polarity and energy metabolism. Physiol Rev 2009;89:777–798.

40. Fu D, Wakabayashi Y, Lippincott-Schwartz J, Arias IM. Bile acid stimulates hepatocyte polarization through a cAMP-epac-MEK-LKB1-AMPK pathway. Proc Natl Acad Sci USA 2011;108:1403–1408.

41. French KR, Pollitt CC. Equine laminitis: Cleavage of laminin 5 associated with basement membrane dysadhesion. Equine Vet J 2004;36:242–247.

42. French KR, Pollitt CC. Equine laminitis: Loss of hemidesmosomes in hoof secondary epidermal lamellae correlates to dose in an oligofructose induction model: An ultrastructural study. Equine Vet J 2004;36:230–235.

43. Lv ZM, Liu Y, Zhang PJ, et al. The role of AMPKalpha in high-glucose-induced dysfunction of cultured rat mesangial cells. Ren Fail 2012;34:616–621.

44. Li X, Song Y, Han Y, et al. Liver X receptor agonist alleviated high glucose-induced endothelial progenitor cell dysfunction via inhibition of reactive oxygen species and activation of AMP-activated protein kinase. Microcirculation 2012;19:547–553.

45. Peeters A, Fraisl P, van den Berg S, et al. Carbohydrate metabolism is perturbed in peroxisome-deficient hepatocytes due to mitochondrial dysfunction, AMP-activated protein kinase (AMPK) activation, and peroxisome proliferator-activated

receptor gamma coactivator 1alpha (PGC-1alpha) suppression. J Biol Chem 2011;286:42162–42179.

46. Chen R, Yang L, McIntyre TM. Cytotoxic phospholipid oxidation products. cell death from mitochondrial damage and the intrinsic caspase cascade. J Biol Chem 2007;282:24842–24850.

47. Corcoran MP, Lamon-Fava S, Fielding RA. Skeletal muscle lipid deposition and insulin resistance: Effect of dietary fatty acids and exercise. Am J Clin Nutr 2007;85:662–677.

48. Eckardt K, Taube A, Eckel J. Obesity-associated insulin resistance in skeletal muscle: Role of lipid accumulation and physical inactivity. Rev Endocr Metab Disord 2011;12:163–172.

49. Kimura N, Tokunaga C, Dalal S, et al. A possible linkage between AMP-activated protein kinase (AMPK) and mammalian target of rapamycin (mTOR) signalling pathway. Genes Cells 2003;8:65–79.

50. Kimball SR, Siegfried BA, Jefferson LS. Glucagon represses signaling through the mammalian target of rapamycin in rat liver by activating AMP-activated protein kinase. J Biol Chem 2004;279:54103–54109.

51. Quinn PG, Yeagley D. Insulin regulation of PEPCK gene expression: A model for rapid and reversible modulation. Curr Drug Targets Immune Endocr Metabol Disord 2005;5:423–437.

52. Lee JM, Seo WY, Song KH, et al. AMPK-dependent repression of hepatic gluconeogenesis via disruption of CREB.CRTC2 complex by orphan nuclear receptor small heterodimer partner. J Biol Chem 2010;285:32182–32191.